



Tuning the Type-2 Fuzzy Controller for Active Control of Buildings Under Seismic Vibrations

Farzaneh Shahabian Moghaddam¹ · Hashem Shariatmadar¹ · Siamak Golnargesi²

Received: 16 May 2022 / Accepted: 25 October 2022
© The Author(s), under exclusive licence to Shiraz University 2022

Abstract

To deal with the prevailing uncertainties in controlling the buildings against earthquake hazard, it is necessary to have a powerful tool. Type-2 fuzzy logic is a growing research topic with much evidence of successful applications to reason with uncertainty, but still not very popular in seismic control problems. Changing T1 fuzzy sets to T2 fuzzy sets automatically doesn't improve the performance. To achieve better performance, one needs to tune and carefully design the type-2 fuzzy parameters. This paper presents the application of interval type-2 fuzzy logic controller (IT2FLC) for active control of a 9-story nonlinear benchmark building. The design of type-1 fuzzy logic controller (T1FLC) is also considered for the purpose of comparison with the IT2FLC. Genetic algorithm (GA) is used to tune T1 and IT2 FLC scaling factors and footprint of uncertainty (FOU) parameters. The performance of the controller is validated through the computer simulation on MATLAB. The use of IT2FLC has successfully reduced the displacement and acceleration time history responses of the structure. Evaluation results show superior performance of IT2FLC for reducing undesirable vibrations and structural damages in compare to T1FLC.

Keywords Seismic vibration · Active control · IT2 fuzzy logic controller · Nonlinear benchmark building · Genetic algorithms

1 Introduction

Reducing structural responses to enhance safety and providing conditions for serviceability and maintenance is one of the goals of researchers. Control tools are very effective in achieving these goals. Structural control methods are classified into several categories including passive, active, semi-active, and hybrid systems. In addition to classical methods, intelligent methods are also used to control the structures. Some of these algorithms, such as optimal control, pole positioning, H₂, and H_∞, are based on mathematical methods, and some others such as fuzzy and neural algorithms,

are intelligent algorithms (Soong 1988; Spencer and Nagarajaiah 2003; Housner 1997; Jung et al. 2004).

Fuzzy logic, introduced by Zadeh (1975), the father of fuzzy logic, enables the use of linguistic directions as a basis for control. The main advantages of using fuzzy control can be its robustness against the uncertainties and errors in the various parts of the control system such as data, loads, structure model, measurements and etc. Another important feature of this method is the ability to use it in nonlinear systems. Due to the nature of nonlinear behavior of structures, this method can be useful for structural control. Using human knowledge and experience in controller design, the possibility of adapting the control system and the mathematical and computational simplicity, can be considered as the other advantages of fuzzy control.

One of the main constraints of type-1 fuzzy systems is their inability to consider uncertainty in fuzzy rules, to overcome this deficiency, Zadeh (1975) introduced more general kinds of fuzzy sets which their membership function grades are themselves fuzzy. The two most widely studied of these are interval-valued fuzzy sets and general type-2 fuzzy sets. For the former, the membership grade is a uniformly

✉ Hashem Shariatmadar
Shariatmadar@um.ac.ir

¹ Department of Civil Engineering, Ferdowsi University of Mashhad, Azadi Square, Mashhad, Islamic Republic of Iran

² Department of Civil Engineering and Environment, Khavaran Institute of Higher Education, Fallahi Square, Mashhad, Islamic Republic of Iran

weighted interval of values, whereas for the latter the membership grade is a non-uniformly weighted interval of values. Obviously, interval-valued fuzzy sets are a special case of general type-2 fuzzy sets and are therefore called interval type-2 fuzzy sets (Wu 2012; Castillo et al. 2016). By 1990, most research in fuzzy systems focused on type-1 fuzzy, and the number of papers on type-2 fuzzy sets was very small. Gradually, research on fuzzy type-2 systems was developed; as Mendel et al. (2014) developed the basic concepts of type-2 fuzzy sets. Liang and Mendel (2000) proposed an effective computational method for calculating operators of type-2 fuzzy sets using the concept of upper and lower membership functions. Karnik and Mendel (2001) provided the entire foundation and framework for singleton type-2 fuzzy systems, including type-reduction and two very widely used algorithms for computing the type-reduced set (the KM and EKM algorithms).

In recent years, extensive research has been done on the use of T1FLC to control the behavior of structures. The T1FLC has been investigated for the active control of civil engineering structures by Faravelli and Yao (1996), Samali et al. (2004), Al-Dawod et al. (2001, 2004), Kang and Kim (2010) and Ahlawat and Ramaswamy (2004). Karamodin et al. (2012) used a genetic-fuzzy control method in order to control the benchmark structure. The comparison between their proposed controller and other controllers shows a significant decrease in the structure response in comparison with other controllers.

However, despite the ability of T2FLC method to deal with issues of high uncertainty, research on the use of these systems in the field of control of structures has been very limited. Golnargesi et al. (2018) studied the seismic control of structures using ATMD with an interval type-2 fuzzy controller. In their research, they showed that, an interval type-2 fuzzy controller significantly reduces the structural response compared with type-1 fuzzy controller. Bathaei et al. (2018) investigated the performance of a semi-active tuned mass damper (TMD) with adaptive magnetorheological (MR) damper using type-1 and -2 fuzzy controllers for seismic vibration mitigation of an 11-degree of freedom building model. Paul et al. (2018) applied a bidirectional active control with type-2 fuzzy PD and PID system to compensate the unknown uncertainties of a two-story building. In Azadvar et al. (2018) research, an interval type-2 fuzzy system has been used to reduce damage in a structure equipped with MR dampers.

The scaling factors in the output and input of T1FL and IT2FL controllers play a vital role in improving the performance of the closed-loop system. However, using trial-and-error procedure for tuning these design parameters is exhaustive, hence an optimization technique is applied to achieve their optimal values and to reach an improved

performance (Humaidi et al. 2021 and Wu et al. 2019). In this study, genetic algorithms (GA) is proposed as a useful tool to tune the parameters of T1 and IT2 FLC. To the best of the author's knowledge, at this moment, this research is the first application of GA-tuned IT2FLC for active control of structures under seismic vibrations.

Yielding and nonlinear behavior is very likely to occur when buildings are subjected to severe wind or earthquake. The linear models do not include disturbances caused by large displacement or material nonlinearity and damage (Azizi et al. 2020). Therefore the main objective of this work is to apply an intelligent controller; an optimal IT2Fuzzy logic controller, to the 9-story benchmark building defined by Ohtori et al. (2004) to handle the nonlinearity of the system. The effectiveness of controllers has been verified via numerical simulations based on MATLAB/Simulink programming software.

2 Interval Type-2 Fuzzy Logic Controller

Interval type-2 fuzzy set (IT2FS) is a more complete form of common type-1 fuzzy sets. In fact, type-1 fuzzy is a subset of type-2 fuzzy set. The most shortcoming of type-1 membership functions is their inability to take uncertainties. To overcome this disadvantage, type-2 fuzzy MF can be used. As shown in Fig. 1, each type-2 MF is composed of a lower membership function and an upper membership function. The space between these two bounding functions is called footprint of uncertainty (FOU), as seen in Fig. 1, FOU overcomes the mentioned deficiency associated with type-1 MFs (Mendel et al. 2014).

In this paper, it has been assumed that the reader is familiar with the basics of fuzzy logic and type-1 fuzzy sets, so that here the focus is entirely on IT2FLS and its advantages over T1FLS. A type-2 fuzzy set \tilde{A} can be defined by its type-2 membership function $\mu_{\tilde{A}}(x, u)$ as:

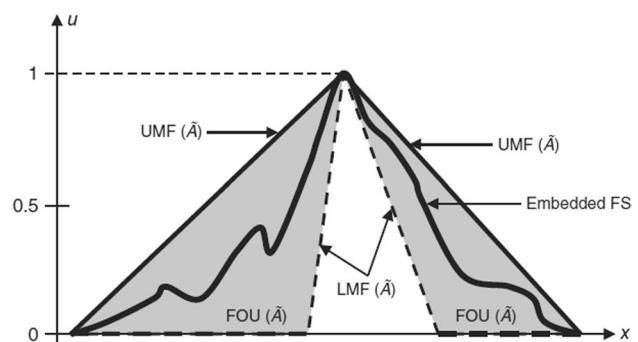


Fig. 1 T2FLC membership function (Mendel et al. 2014)

$$\tilde{A} = \int \int_{x \in X, u \in J_x} \frac{\mu_{\tilde{A}}(x, u)}{(x, u)} \quad (1)$$

which is often referred to as the point-valued representation of a T2 FS and is useful as a starting point. where $x \in X$, $u \in J_x \subseteq [0, 1]$, and X represents the universe of the primary variable x of \tilde{A} . The secondary MF of \tilde{A} is also called a vertical slice:

$$\mu_{\tilde{A}}(x = x', u) \equiv \mu_{\tilde{A}}(x') = \int_{u \in J_{x'}} \frac{f_{x'}(u)}{u} \quad (2)$$

where $0 \leq f_{x'}(u) \leq 1$. In the case of IT2FLS the secondary membership grades all equal 1, that is to say, for any $x = x'$, $f_{x'}(u) \equiv 1$.

The FOU is uncertainty in the primary membership grades of a type-2 MF, which consists of a bounded region; the UMF is a subset that has the maximum membership grade of the FOU, and the LMF is a subset that has the minimum membership grade of the FOU. The two-dimensional $\mu_{\tilde{A}}(x, u)$ is referred to as the footprint of uncertainty (FOU) of \tilde{A} :

$$FOU(\tilde{A}) = \bigcup_{x \in X} J_x = \{ (x, u) | u \in J_x \subseteq [0, 1] \} \quad (3)$$

where J_x is the primary membership of \tilde{A} ; here the lower MF (LMF) $\mu_{\tilde{A}}^-(x)$ and the upper MF (UMF) $\mu_{\tilde{A}}^+(x)$ comprise the FOU, where:

$$\mu_{\tilde{A}}^-(x) = LMF(\tilde{A}) = \inf \{ u | u \in [0, 1], \mu_{\tilde{A}}(x, u) \geq 0 \} \quad (4)$$

and,

$$\mu_{\tilde{A}}^+(x) = UMF(\tilde{A}) = \sup \{ u | u \in [0, 1], \mu_{\tilde{A}}(x, u) \geq 0 \} \quad (5)$$

A typical IT2FLC consists of five parts as fuzzifier, rule base, inference engine, type-reducer, and defuzzifier. The process of type reduction is usually performed by the most popular computationally intensive Karnik–Mendel (KM) iterative algorithms proposed by Wu and Mendel (2010). In order to perform COS type-reduction one begins with the firing intervals for the rules $\left[\begin{matrix} f^i(x') \\ - \end{matrix}, \bar{f}^i(x') \right]$, which can be determined by either minimum or product t-norm. Instead of combining them directly with their respective consequent FOU they are combined with the centroid of their respective consequent FOU, $[c_p^i, c_r^i]$. Let $u_{COS}(x)$ denote the Cos type reduced set, where:

$$u_{COS}(x) = u_{IWA}(x') = 1 / [u_l(x), u_r(x)] \quad (6)$$

During an interval weighted average (IWA) process, using KM algorithms, $u_l(x), u_r(x)$ are calculated. After designing an IT2 Mamdani fuzzy system, the centroid of each rule's consequent set, c_p^i, c_r^i , only has to be computed once (and then stored), because those centroids do not depend upon the input to the fuzzy system. At the second step, the defuzzifier turns the type-1 fuzzy set to a crisp value by the means of averaging (Mendel 2014):

$$u(x) = \frac{1}{2} [u_l(x) + u_r(x)] \quad (7)$$

In Fig. 2, block diagram summary of IT2Mamdani FLC computations that use COS type reduction and average defuzzification is illustrated.

3 Numerical Study

3.1 Structural Model

Third-generation benchmark control problems for seismically excited nonlinear buildings are an effort to evaluate the developed control strategies in order to apply them in field applications and systematically evaluate the performance of various control strategies, especially in the case of nonlinear building structures. The 9-story benchmark building used for this study was designed for the Los Angeles region as defined by Ohtori et al. (2004). The 9-story benchmark structure is 45.75 m by 45.73 m in width and 37.19 m in height. The bays are 9.15 m on center, in both directions, with five bays each in the N–S and E–W directions. The lateral load resisting system of the building is comprised of steel perimeter MRFs with simple framing on the furthest south E–W frame. The interior bays of the structure contain simple framing with composite floors. The details of this structure are shown in Fig. 3. For more details refer to the problem definition paper Ohtori et al. (2004).

3.2 Nonlinear Model

During large seismic events, structural members can yield, resulting in a nonlinear response behavior that may be significantly different than a linear approximation. To better represent the nonlinear behavior, a bilinear hysteresis model, as shown in Fig. 4, is used to model the plastic hinges, the points of yielding, of the 9-story building structural members. The bilinear bending properties are predefined for each structural member. These plastic hinges, which are assumed to occur at the moment resisting column–beam and column–column connections, introduce a material nonlinear

Fig. 2 Block diagram summary of IT2Mamdani FLC computations that use COS TR (Mendel et al. 2014)

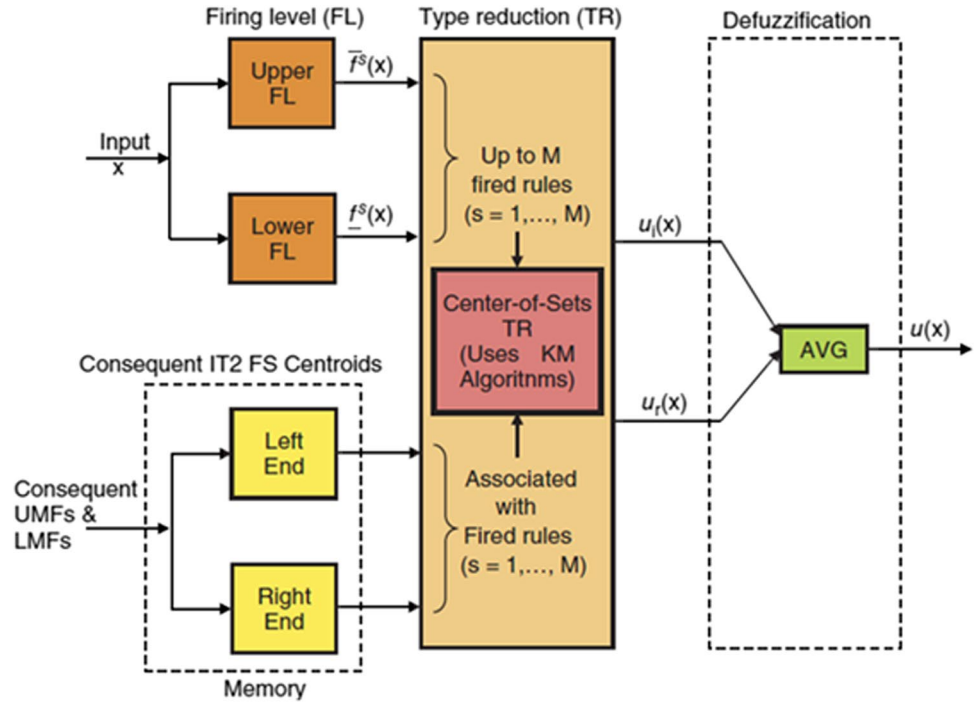
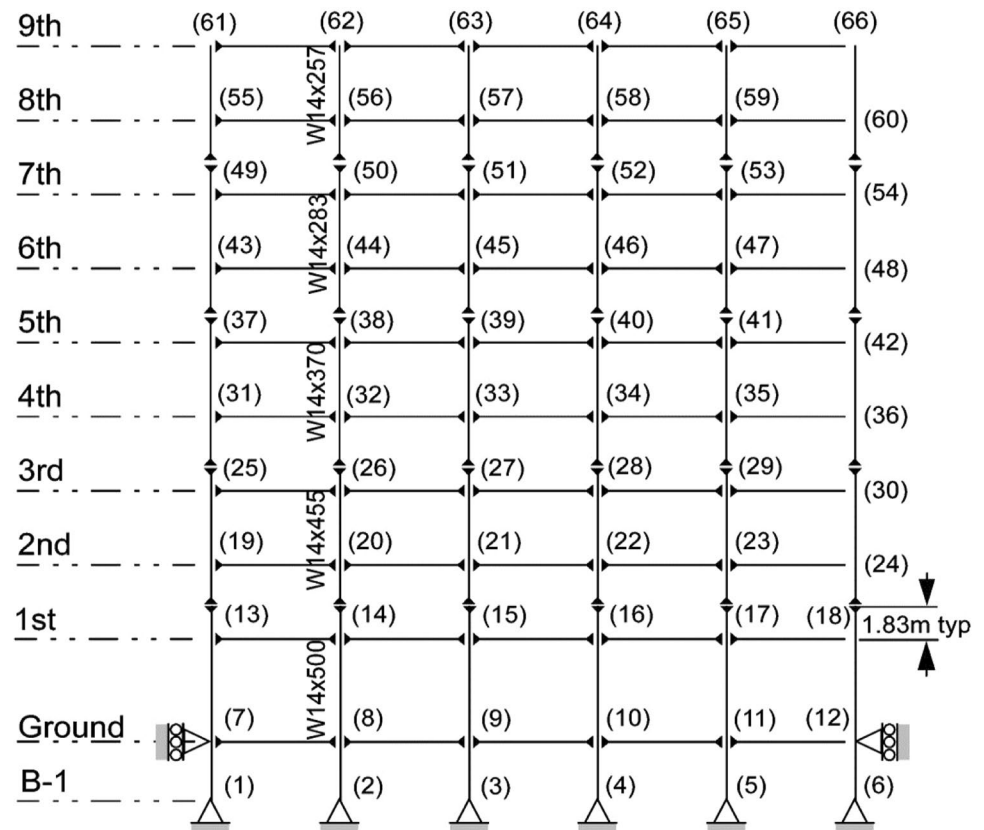


Fig. 3 Nine-story benchmark building, north-south moment-resisting frame (Ohtori et al. 2004)



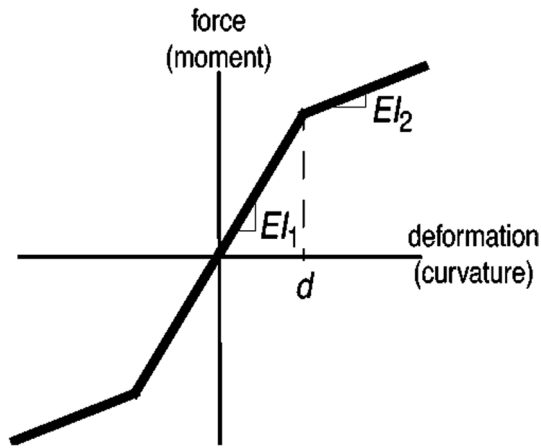


Fig. 4 Bilinear hysteresis model for structural member bending (Ohtori et al. 2004)

behavior of these structures. For more details refer to the problem definition paper Ohtori et al. (2004).

3.3 Ground Motion Records

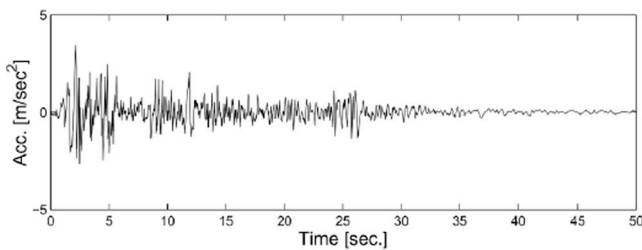
To investigate the effectiveness of the control system, two far-field and two near-field historical ground motion records are selected:

- *El Centro* The N–S component recorded at the Imperial Valley Irrigation District substation in El Centro, California, during the Imperial Valley, California, earthquake of May 18, 1940.
- *Hachinohe* The N–S component recorded at Hachinohe City during the Tokachi-oki earthquake of May 16, 1968.
- *Northridge* The N–S component recorded at Sylmar County Hospital parking lot in Sylmar, California, during the Northridge, California earthquake of January 17, 1994.
- *Kobe* The N–S component recorded at the Kobe Japanese Meteorological Agency station during the Hyogo-ken Nanbu earthquake of January 17, 1995.

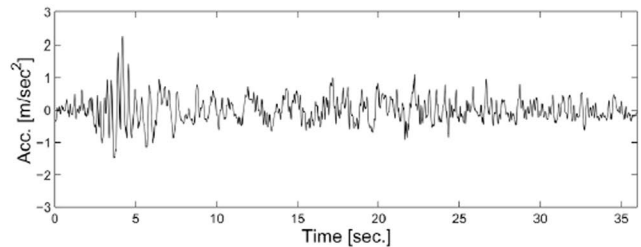
The basic principles and specifications of these records are presented in Table 1. The selected ground motion records

Table 1 Characteristics of the selected earthquake records

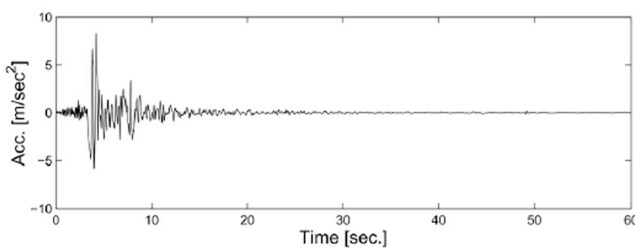
Earthquake -Date	M_w	R (km)	Station	Component	PGA(g)	PGW (cm/s)	PGD (cm)
Elcentro-1940	6.9	–	Irrigation District	EI-180	0.3483	38.11	232.61
Hachinohe-1968	7.8	–	Hachinohe	S252-NS	0.2294	40.63	172.09
Northridge-1994	6.7	9.9	Sylmar County Hospital	Sylmar-360	0.8426	128.91	30.65
Kobe-1995	6.9	0.96	Meteorological Agency	KJMA-000	0.8336	92.09	234.79



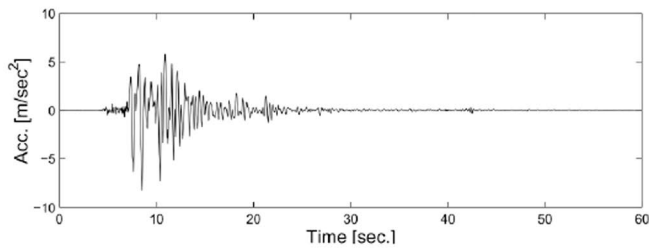
(a) El Centro



(b) Hachinohe



(c) Northridge



(d) Kobe

Fig. 5 Time histories of the near- and far-field historical earthquake records used in the benchmark study (Ohtori et al. 2004)

cover a moment magnitude (M_w) range from 6.7 to 7.8 while for near-field earthquakes, the distance (R) to the active fault varies from 0.96 to 9.9 km. The Peak Ground Acceleration (PGA), the Peak Ground Velocity (PGV) and the Peak Ground Displacement (PGD) are also presented for each record. The absolute peak acceleration of the earthquake records is 3.417, 2.250, 8.2676, and 8.1782 m/s^2 , respectively. The earthquake records are shown in Fig. 5. Additionally, this benchmark study will consider various levels of each of the earthquake records including: 0.5, 1.0, and 1.5 times the magnitude of El Centro and Hachinohe; and 0.5 and 1.0 times the magnitude of Northridge and Kobe. This is a total of ten earthquake records to be considered in the evaluation of each control strategy (Ohtori et al. 2004).

3.4 Control Strategy

Design of a control system includes specifications and location of the sensors, specification and location of the control devices, and a controller to determine the control action from the measured responses. Relative displacement and velocity information of different floors have been used as feedback to the FLC measured by sensors located on each floor. The size of the actuators is limited to provide a maximum control force of 1000 kN where actuators with this capacity are readily available. Each actuator is implemented in the structure using a chevron brace configuration, in which the actuator is horizontal and rigidly attached between two consecutive levels of the building. Thus, the actuators placed on the first level will produce equal and opposite control forces on the first and second floors. Although there are multiple control devices acting on some floors, it is assumed that all control devices on a single floor experience the same inputs and respond in the same way. For the 9-story building, a total of 12 actuators have been used, two at the first, second and third floor and one on each of the other floors. The time interval for all operation was 0.01 s.

To design a fuzzy system, input, output, membership functions, and fuzzy rules must be determined. These parameters can be determined by the knowledge of an expert or by conventional methods. In this research, the general

Table 2 Specifications of T1 and IT2 FLC

	T1	IT2
Fuzzification	singleton	singleton
Aggregation	Product t-norm	Product t-norm
Fuzzy Inference	Mamdani	Mamdani
Type Reducer		Center of sets
Defuzzification	Center of sets	average

Table 3 Fuzzy linguistic variables

NL	Large Negative Value
N	Negative Value
Z	Zero Value
P	Positive Value
PL	Large Positive Value

structure of the system, including input and output variables, the number and type of membership functions and fuzzy rules, are determined based on the knowledge and experience of authors. In some cases, system was modified iteratively, while trying to obtain optimality. The input values correspond to the relative displacement and velocity of each floor of the structure and the output values are related to the amount of force applied to the structure. The Specifications of T1FLC and IT2FLC are given in Table 2 and the abbreviation's description of fuzzy variables is shown in Table 3. As shown in Table 3, for each variable, five values are used.

The fuzzy inference engine consists from set of rules which are given in Table 4. The membership functions chosen for the input and output variables are triangular shaped, for simplicity, and which relieve the computational burden as illustrated in Figs. 6, 7. As illustrated in Fig. 7, FOU parameters are H and M and would be optimized by GA. Notice that inputs and the output variables are normalized to $[-1, 1]$ by the use of scale factors which are achieved by GA optimization method. The control strategy based on T1 and IT2FLS was implemented in MATLAB through the author's m-file written in Simulink. No fuzzy logic toolboxes have been used either for T1 or IT2 fuzzy operation.

3.5 Evaluation Criteria

The performance of the controller is investigated based on the evaluation criteria (J1–J14) specified for the nonlinear benchmark buildings. The evaluation criteria are divided into three categories: Building responses, building damage and control devices. These three categories have both peak-and normed-based criteria. Small values of the evaluation criteria are generally more desirable. These criteria

Table 4 Fuzzy associative memory

Relative velocity	Control force				
	Relative displacement				
	NL	N	Z	P	PL
NL	pl	pl	p	Z	N
N	PL	PL	P	Z	N
Z	PL	PL	Z	N	NL
P	PL	PL	Z	NL	NL
PL	PL	P	N	NL	NL

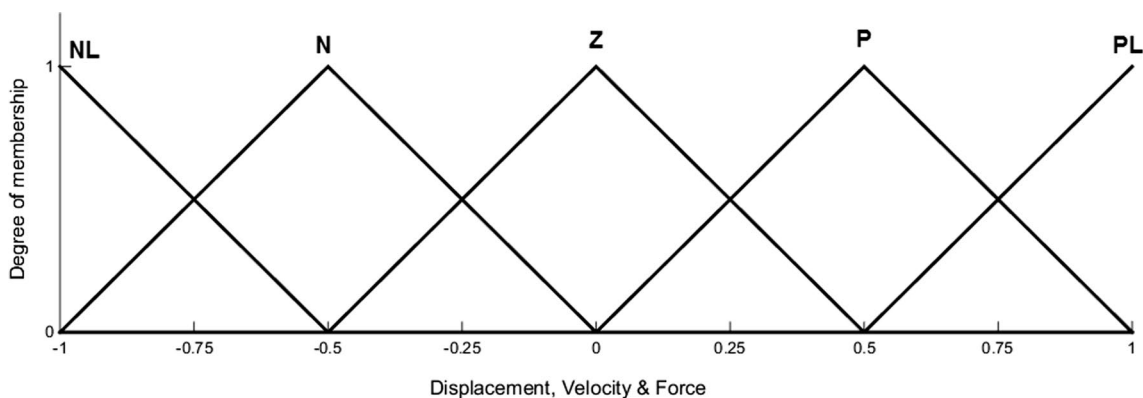


Fig. 6 T1 MFs for input and output variables

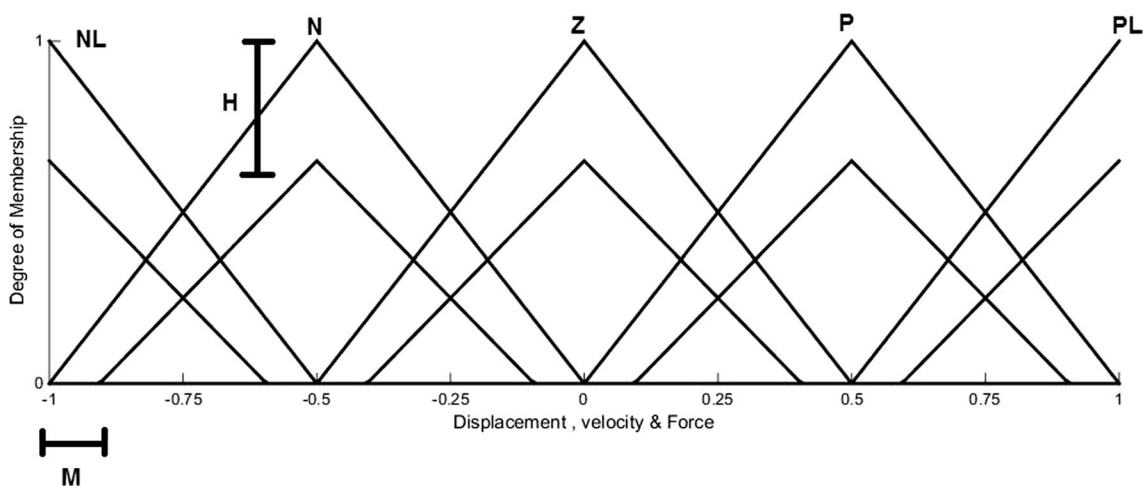


Fig. 7 IT2 MFs for input and output variables

are calculated as a ratio of the controlled and uncontrolled responses. The first category of the evaluation criteria is related to the building responses. The first three criteria are based on peak interstory drift ratio ($J1$), level acceleration ($J2$), and base shear ($J3$). The next three criteria are based on normed building responses. The interstory drift ($J4$), level acceleration ($J5$), and base shear ($J6$) are defined in their normed-based forms. where the norm $\|\cdot\|$ is computed using the following equation:

$$\|\cdot\| = \sqrt{\frac{1}{t_f} \int_0^{t_f} [\cdot]^2 dt} \tag{8}$$

t_f is sufficiently a large time to allow the response of the structure to attenuate. In this benchmark study, the duration of 100 s is adopted for the El Centro, Hachinohe, and Northridge earthquakes and 180 s for the Kobe earthquake.

The second category of the evaluation criteria assesses the building damage. These criteria have been added because of

the nonlinear character of this benchmark study. Both ends of each element are considered in these criteria to assess the yielding, excluding simply supported beam elements as well as the fixed hinged beam elements. The seventh and eighth evaluation criteria are based on peak responses while the ninth and tenth are normed-based criteria. The evaluation criteria for the ductility factor ($J7$) and dissipated energy of the curvatures at the end of members ($J8$). The ninth evaluation criterion ($J9$) is the ratio of the plastic connections sustained by the structure while controlled and uncontrolled. Evaluation criteria $J8$ and $J9$ only have meaning for structures undergoing plastic deformations and are, therefore, undefined (should not be calculated or reported) when the uncontrolled building remains elastic.

The third category is related to the control devices. This category assesses the required performance of the devices. Peak criterion $J11$, $J12$, and $J13$ show control force, control device stroke, and power used for control. The fourteenth evaluation criterion ($J14$) is a measure of the total power

Table 5 Summary of evaluation criteria for the nonlinear benchmark problem

Interstory drift ratio	Level acceleration	Base shear
$J1 = \max \left\{ \frac{\max_{i,j} d_i(t) }{h_i} \right\}$	$J2 = \max \left\{ \frac{\max_{i,j} \ddot{x}_{ai}(t) }{\ddot{x}_a^{\max}} \right\}$	$J3 = \max \left\{ \frac{\max_{i,j} \sum_i m_i \ddot{x}_{ai}(t) }{F_b^{\max}} \right\}$
Normed Interstory Drift Ratio	Normed level Acceleration	Normed base Shear
$J4 = \max \left\{ \frac{\max_{i,j} \frac{\ d_i(t)\ }{h_i}}{\ \delta^{\max}\ } \right\}$	$J5 = \max \left\{ \frac{\max_{i,j} \ \ddot{x}_{ai}(t)\ }{\ \ddot{x}_a^{\max}\ } \right\}$	$J6 = \max \left\{ \frac{\ \sum_i m_i \ddot{x}_{ai}(t)\ }{\ F_b^{\max}\ } \right\}$
Ductility	Dissipated Energy	Plastic Connections
$J7 = \max \left\{ \frac{\max_{i,j} \frac{ \varphi_j(t) }{\varphi_{yj}}}{\varphi^{\max}} \right\}$	$J8 = \max \left\{ \frac{\max_{i,j} \frac{\int dE_j}{F_{yj} \varphi_{yj}}}{E^{\max}} \right\}$	$J9 = \max \left\{ \frac{N_d^c}{N_d} \right\}$
Normed Ductility	Control Force	Control Device stroke
$J10 = \max \left\{ \frac{\max_{i,j} \frac{\ \varphi_j(t)\ }{\varphi_{yj}}}{\ \varphi^{\max}\ } \right\}$	$J11 = \max \left\{ \frac{\max_{i,j} f_l(t) }{w} \right\}$	$J12 = \max \left\{ \frac{\max_{i,j} y_l^d(t) }{x^{\max}} \right\}$
Control Power	Normed Control Power	
$J13 = \max \left\{ \frac{\max_{i,j} [\sum_l p_l(t)]}{\ddot{x}_a^{\max} W} \right\}$	$J14 = \max \left\{ \frac{\sum_l \frac{1}{l_j} \int_0^{t_j} p_l(t)}{\ddot{x}_a^{\max} W} \right\}$	

$i = [1, 9]$

$d_i(t)$ = interstory drift of the above ground level over the time history of each earthquake (m)

h_i = height of each of the associated stories (m)

δ^{\max} = maximum interstory drift ratio of the uncontrolled structure

$\ddot{x}_{ai}(t)$ = absolute acceleration of the i -th level with control devices (m/sec²)

\ddot{x}_a^{\max} = absolute acceleration of the i -th level without control devices (m/sec²)

m_i = seismic mass of the i -th above ground level (kg)

F_b^{\max} = maximum base shear of the uncontrolled structure for each respective earthquake (N)

φ_j = curvature at the ends of the j -th element (member)

$\int dE_j$ = dissipated energy at the ends of the member during the respective earthquake

φ_{yj} = yield curvature at the end of the j -th member

F_{yj} = yield moment at the end of the j -th member

φ^{\max} = maximum curvatures (maximum of all element ends and over time) of uncontrolled structure

E^{\max} = maximum dissipated energy (maximum of all element ends and over time) of uncontrolled structure

N_d = number of damaged connections (member ends) without control

N_d^c = number of damaged connections with control.

$f_l(t)$ = force generated by the l -th control device over the time history of each earthquake (N)

W = seismic weight of the building based on the above ground mass of the structure (N)

$y_l^d(t)$ = displacement across the l -th control device during the earthquake (m).

x^{\max} = maximum uncontrolled displacement of the levels relative to the ground (m)

$p_l(t)$ = power required by the l -th control device. (For active control devices $p_l(t) = |y_l^d(t) \dot{f}_l(t)|$, where $\dot{y}_l^d(t)$ = velocity across the l -th control device)

\dot{x}^{\max} = maximum uncontrolled velocity of the levels relative to the ground (m/sec)

required for the control of the structure. A summary of the evaluation criteria is presented in Table 5.

3.6 Genetic Algorithms and Optimization of FLC

The goal of GA optimization in this research is to determine the scaling factors of the IT2 FLC to achieve a desirable control performance. The basic principles of genetic algorithms

(GAs) were first proposed by Holland (1992). GAs are general purpose search algorithms which use principles inspired by natural genetics to evolve solutions to problems. Figure 8 contains the flowchart of a basic GA. A GA starts with a population of randomly generated chromosomes, and advances toward better chromosomes by applying genetic operators modeled on the genetic processes occurring in nature. The population undergoes evolution in a form of

natural selection. During successive iterations, called generations, chromosomes in the population are rated for their adaptation as solutions, and on the basis of these evaluations, a new population of chromosomes is formed using a selection mechanism and specific genetic operators such as crossover and mutation. An evaluation or fitness function must be devised for each problem to be solved. Although there are many possible variants of the basic GA, the fundamental underlying mechanism consists of three operations: evaluation of individual fitness; formation of a gene pool (intermediate population) through a selection mechanism; and recombination through crossover and mutation operators (Gómez-Skarmeta and Jiménez 1999).

Finding the best solution among all feasible solutions is called the optimization problem. In this paper, the optimization problem is considered as a single objective problem while the objective function is formulated based on the non-linear responses of the structure. The general state of the objective function is as following (Azizi et al. 2019):

$$Obj = \frac{\sum_{i=1}^n W_i \frac{CR_i}{UR_i}}{\sum_{i=1}^n W_i} \quad (9)$$

where W_i is the weighing coefficient of the objective function that is considered as the absolute peak accelerations of the selected earthquakes and the summation is utilized for the selected earthquake records. UR_i and CR_i are the uncontrolled and controlled responses of the building. The responses can be chosen based on any of the evaluation criteria discussed in Sect. 3.5. In this paper, the objective function is formulated based on the peak inter-story drift ratio (J_1). It should be noted that all of the J_s can be considered as the building major response in formulation of the objective function; however, in this paper the inter-story drift ratio is selected based on the great importance of this ratio in all seismic design codes and practices (Rahgozar et al. 2022). The mentioned objective function is considered as follows:

$$Obj = \frac{0.34 \times (J_1)_{Elc} + 0.22 \times (J_1)_{Hach} + 0.84 \times (J_1)_{North} + 0.83 \times (J_1)_{Kobe}}{(0.34 + 0.22 + 0.84 + 0.83)} \quad (10)$$

Fuzzy systems possess several parameters that can be optimized (Shariatmadar and Razavi 2014). For example, tuning of the scaling functions, fuzzy membership functions and fuzzy rules are some important tasks in fuzzy system design. Scaling functions applied to the input and output variables of a fuzzy system normalize the universes of discourse in which the fuzzy membership functions are defined. Usually, the scaling functions are parameterized by a single scaling factor or a lower and upper bound in the case of linear scaling (Pourzeynali et al. 2007). In this paper the rules and membership functions are kept fixed and in the case of T1FLC, the scaling factors are optimized. The main characteristic of T2FLC is that its MFs are fuzzy. Therefore, it has more degrees of freedom in designing varieties of systems with uncertainties, for the IT2FLC six parameters are optimized, which are scaling factors and FOU characteristics as depicted in Fig. 7. In the GA tournament some GA operator parameters are very important in improving the GA tournament. One of these parameters is the crossover probability which is taken as 80%. The GA optimization is operated by MATLAB/optimtool. The GA convergence is depicted in Figs. 9, 10.

4 Numerical Results and Discussion

The performance of the fuzzy controller is checked according to the evaluation criteria specified (J_1 – J_{14}) for 9 story nonlinear benchmark building. In order to evaluate the effectiveness of the proposed control system in managing the uncertainties governing the structure, the uncontrolled structure response and controlled structure equipped with type-1

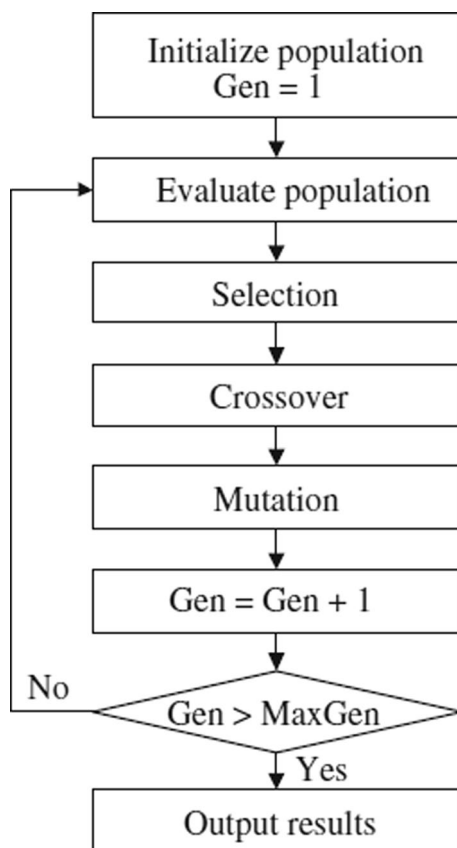


Fig. 8 The flowchart of a basic GA

fuzzy controller, have been investigated too. In Tables 6, 7, evaluation criteria has been reported for T1 and IT2FLC, respectively. By reviewing Tables 6, 7, it can be concluded that with a same FLC construction (Rule base and MFs) and control features (number and place of sensors and actuators),

IT2FLC showed a better performance than the T1FLC in almost all criteria. The results show the ability of the optimized IT2 fuzzy controller to reduce J1 to J6 (building response) for far field earthquakes up to 30% and for Kobe up to 15% in contrast with T1 fuzzy controller and comprise

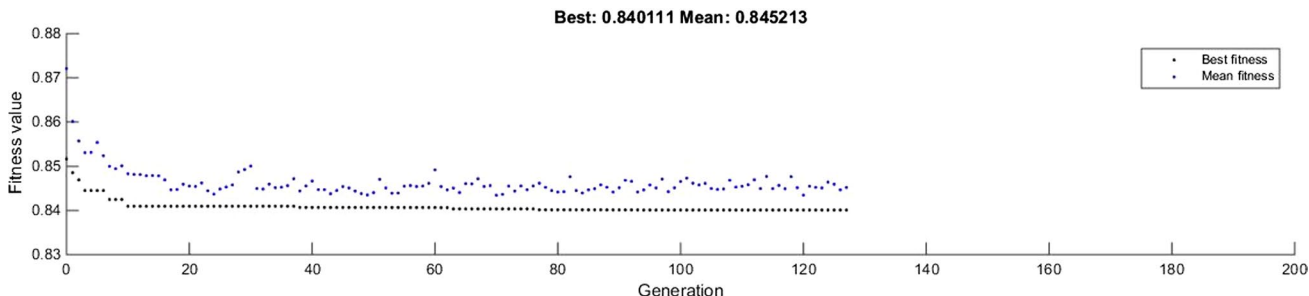


Fig. 9 The convergence history of GA optimization for T1 FLC

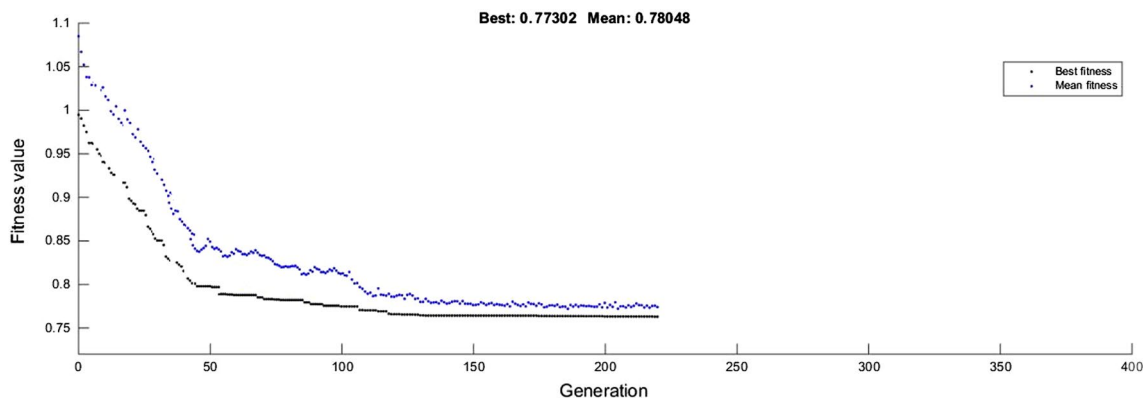


Fig. 10 The convergence history of GA optimization for IT2 FLC

Table 6 Earthquake evaluation criteria for T1FLC of 9-story benchmark structure

Earthquake (intensity)	El Centro			Hachinohe			Northridge		Kobe	
	0.5	1.0	1.5	0.5	1.0	1.5	0.5	1.0	0.5	1.0
J1	0.701	0.805	0.918	0.699	0.745	0.690	0.890	0.985	0.726	0.959
J2	0.713	0.825	0.884	0.753	0.739	0.920	1.000	0.950	0.958	0.959
J3	0.760	0.947	1.000	0.710	0.848	0.900	1.000	1.080	0.879	0.998
J4	0.522	0.624	1.029	0.792	0.816	0.662	0.857	1.278	0.617	1.123
J5	0.641	0.620	0.654	0.926	0.791	0.856	0.760	0.801	0.683	0.822
J6	0.595	0.744	0.810	0.807	0.853	0.904	0.740	0.796	0.699	0.876
J7	0.742	0.735	0.897	0.704	0.583	0.814	0.854	1.017	0.648	0.945
J8	–	0.429	0.602	–	0.018	0.617	0.418	0.868	0.205	0.636
J9	–	0.653	0.957	–	0.140	0.775	0.905	0.907	0.654	1.000
J10	0.572	0.686	1.170	0.789	0.669	0.566	1.100	0.948	0.748	0.911
J11	0.011	0.011	0.011	0.011	0.011	0.011	0.011	0.011	0.011	0.011
J12	0.165	0.173	0.196	0.144	0.146	0.156	0.168	0.163	0.202	0.215
J13 × 10 ⁻³	5.66	8.67	12.7	4.39	7.93	14.4	11.2	14	12.6	18.4
J14 × 10 ⁻⁴	1.78	2.95	4.62	2.15	3.45	6.26	3.10	3.17	2.16	2.66

Table 7 Earthquake evaluation criteria for IT2FLC of 9-story benchmark structure

Earthquake (intensity)	El Centro			Hachinohe			Northridge		Kobe	
	0.5	1.0	1.5	0.5	1.0	1.5	0.5	1.0	0.5	1.0
J1	0.587	0.647	0.798	0.507	0.564	0.626	0.817	0.940	0.582	0.930
J2	0.632	0.660	0.809	0.600	0.627	0.920	1.000	0.950	0.832	0.947
J3	0.587	0.822	1.000	0.528	0.659	0.900	1.000	1.080	0.792	0.964
J4	0.385	0.484	0.920	0.620	0.680	0.588	0.634	0.930	0.274	0.932
J5	0.585	0.464	0.542	0.877	0.632	0.771	0.670	0.779	0.575	0.769
J6	0.448	0.604	0.732	0.641	0.721	0.833	0.636	0.753	0.605	0.844
J7	0.572	0.500	0.778	0.497	0.430	0.734	0.719	0.944	0.507	0.913
J8	–	0.004	0.406	–	0.000	0.390	0.232	0.737	0.063	0.545
J9	–	0.061	0.725	–	0.000	0.676	0.889	0.907	0.615	1.000
J10	0.422	0.411	1.098	0.616	0.553	0.444	0.883	1.303	0.316	0.666
J11	0.011	0.011	0.011	0.011	0.011	0.011	0.011	0.011	0.011	0.011
J12	0.126	0.139	0.178	0.105	0.111	0.143	0.154	0.157	0.162	0.209
J13 $\times 10^{-3}$	6.25	9.32	13.5	8.66	11.1	16.7	12.7	15	16.9	21.6
J14 $\times 10^{-4}$	2.09	3.77	6.22	2.81	4.79	9.07	3.80	4.15	2.85	3.50

almost same answers for Northridge earthquake. In comparison with the uncontrolled structure response, according to Table 6 the optimized IT2 fuzzy controller reduced J1 to J6 for far field earthquakes up to 50% and for nearfield up to 10% in most cases.

The second category of the evaluation criteria assesses the building damage. These criteria have been added because of the nonlinear character of this benchmark structure. Both ends of each element are considered in these criteria to assess the yielding. Evaluation criteria J8 and J9 only have meaning for structures undergoing plastic deformations and are, therefore, undefined (should not be calculated or reported) when the uncontrolled building remains elastic presented with dash lines in Tables 5, 6. The evaluation criteria for the ductility factor (J7) is reduced up to 30% for far field and 10% for near field in contrast with T1 and up to 60% and 10% for far and near field, respectively, in contrast with uncontrolled structure. From Table 6, dissipated energy of the curvatures at the end of members (J8) and the ratio of the plastic connections sustained by the structure while controlled and uncontrolled (J9) is obtained almost zero for far field earthquakes and that is 100% improvement. The tenth evaluation criterion (J10) is the normed ductility factor, improved about 40% for far field and Kobe earthquakes but increased for about 30% for Northridge earthquake. The comparing results of the maximum curvature and energy dissipation at the ends of structural members prove that the structure with optimized IT2FLC is very well capable of withstanding severe earthquakes.

The third category of criteria is related to the control devices. J11 indicating max control force is the same for T1 and IT2 because of maximum capacity of actuators. Control device stroke (J12) improved up to 25% for far field and had

almost no changes for near field earthquakes in contrast to T1. J13 and J14 criteria indicating power required for the control increased up to 40% for IT2 FLC in contrast to T1.

To assess the effectiveness of the proposed controller, the time history of displacement and acceleration of the 9th floor are also examined. Graphs in Figs. 11, 12, 13, 14 represent comparison of displacement and acceleration time history responses of 9th floor for T1 and IT2 control systems when subjected to far field earthquakes. It is observed carefully that IT2FLC has been able to optimally reduce the displacement and acceleration time history responses in comparison with T1FLC, when the structure subjected to far field earthquakes.

The structural performance of a building is checked from two points of view, structural safety and residential comfort. Therefore, the peak inter-story drift (J1) and base shear force (J3) as indexes of building's damage and maximum level acceleration of stories (J2) as an index of comfort level are of importance to estimate the proposed control performance. To better demonstrate these important criteria bar graphs in Figs. 15, 16, 17 have been illustrated. It is observed that with the use of the proposed controller, human comfort (J2) and safety level (J1, J3) of the structure are both very well guaranteed for far field earthquakes, modest for Kobe which is a double pulse nearfield earthquake and almost weak for Northridge representing a single pulse nearfield earthquake.

5 Conclusions

In recent years, type-2 fuzzy controllers have been used successfully to deal with uncertainties in many real-world applications. Despite the inevitable uncertainties involved in seismic control of buildings, type-2 fuzzy approach is

Fig. 11 Displacement time history of the 9th story for Elcentro earthquake

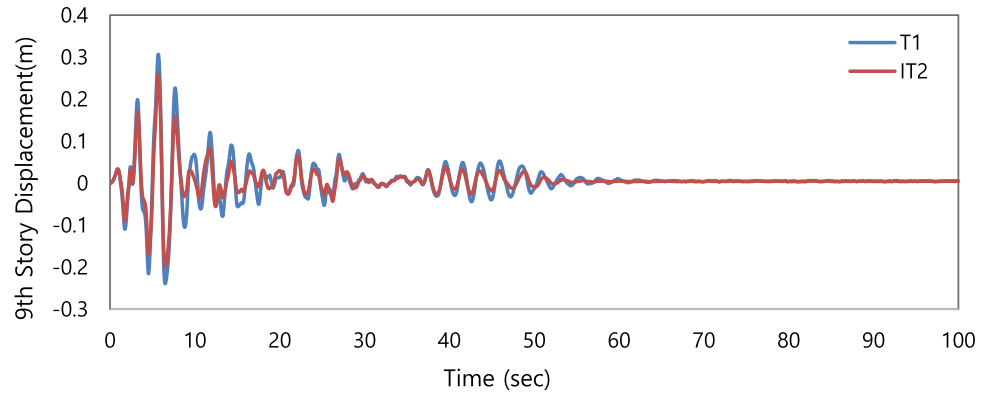


Fig. 12 Acceleration time history of the 9th story for Elcentro earthquake

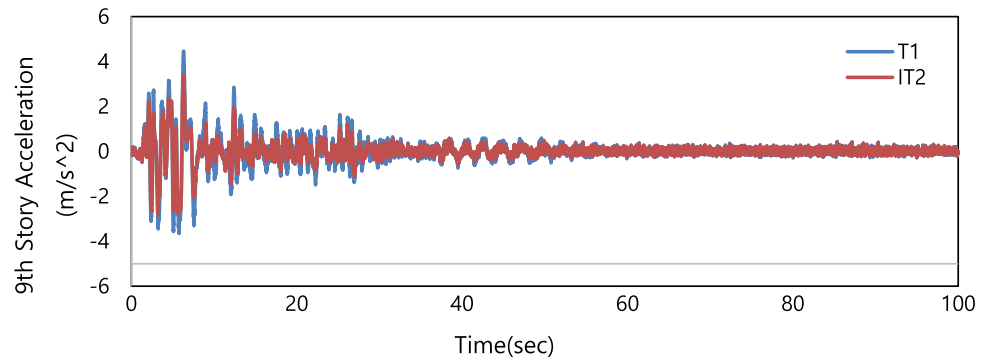


Fig. 13 Displacement time history of the 9th story for Hachinohe earthquake

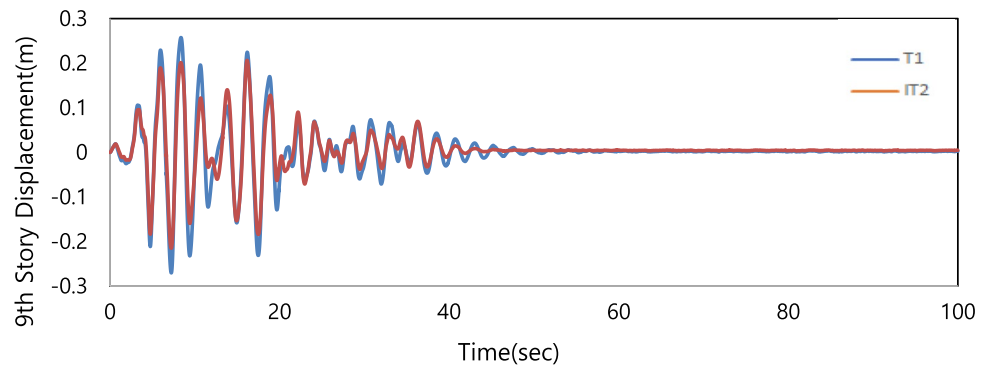
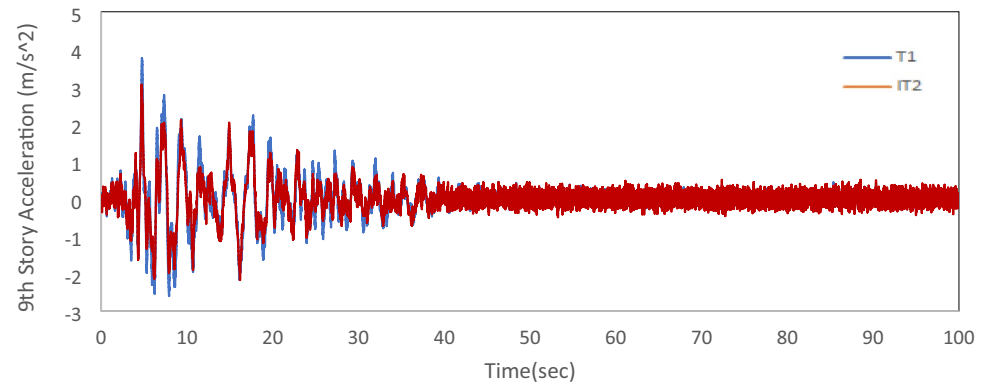


Fig. 14 Acceleration time history of the 9th story for Hachinohe earthquake



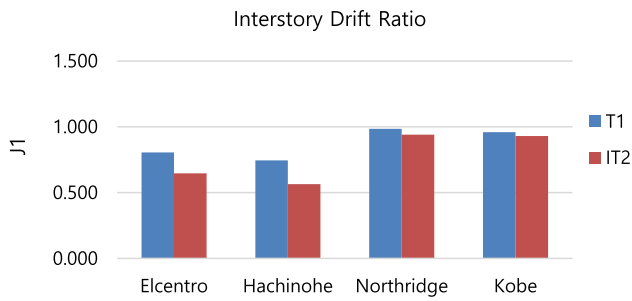


Fig. 15 comparison of J1 for T1 and IT2 for proposed earthquakes with unit intensity

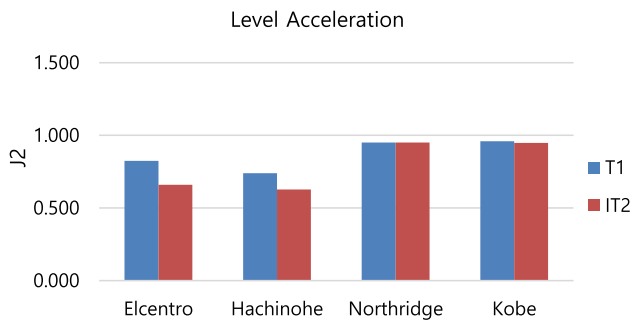


Fig. 16 comparison of J2 for T1 and IT2 for four proposed earthquakes with unit intensity

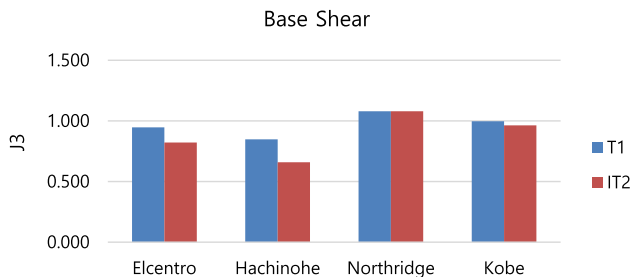


Fig. 17 comparison of J3 for T1 and IT2 for four proposed earthquakes with unit intensity

still abandoned among most researchers in this field. Having more degrees of design freedom, while a great advantage, also complicates matters. It should be known that for achieving desired answers by type-2 fuzzy controller, one must tune and design its parameters very carefully. This problem of tuning can be solved by using optimization methods. Genetic Algorithms (GA) was employed to find optimum fuzzy controller scale factors and FOU parameters. For GA approach the choice of objective function

is of great importance. The objective function was formulated based on the peak inter-story drift ratio. Drift ratio was selected due to the great importance of this ratio in all seismic design codes and practices. The IT2 controller adopted here was chosen not to be a completely optimal one, but only some features to be tuned due to simplicity and time cost and to be comparable with counterpart T1 controller. In order to evaluate the effectiveness of the proposed control system, a T1FLC has been designed too. The performance of the fuzzy controllers was checked against four earthquake records with different intensity therefore the total of ten earthquake records were used in the simulations. The efficiency of the fuzzy controller was checked through a number of evaluation criteria specified for the benchmark study. Although the objective function was formulated based on the peak inter-story drift ratio, but almost all structural performance criteria were effectively improved too. By comparing the results of the IT2 controller with T1FLC, it could be concluded that the IT2 FLC is very powerful in preventing damages of structural members and more effective in reducing the building responses. Finally, by considering the generality issues of the proposed controller, it can be concluded that tuning the IT2FLC parameters, makes it capable of providing very encouraging results in the field of active structural control.

References

- Ahlatw A, Ramaswamy A (2004) Multiobjective optimal fuzzy logic controller driven active and hybrid control systems for seismically excited nonlinear buildings. *J Eng Mech* 130(4):416–423. [https://doi.org/10.1061/\(ASCE\)0733-9399\(2004\)130:4\(416\)](https://doi.org/10.1061/(ASCE)0733-9399(2004)130:4(416))
- Aldawod M et al (2001) Active control of along wind response of tall building using a fuzzy controller. *Eng Struct* 23(11):1512–1522. [https://doi.org/10.1016/S0141-0296\(01\)00037-2](https://doi.org/10.1016/S0141-0296(01)00037-2)
- Al-Dawod M et al (2004) Fuzzy controller for seismically excited nonlinear buildings. *J Eng Mech* 130(4):407–415. [https://doi.org/10.1061/\(ASCE\)0733-9399\(2004\)130:4\(407\)](https://doi.org/10.1061/(ASCE)0733-9399(2004)130:4(407))
- Azadvar M et al (2018) structural damage control with interval type-2 fuzzy logic controller. *AUT J Civ Eng* 2(2):125–134. <https://doi.org/10.22060/AJCE.2018.13827.5255>
- Azizi M et al (2019) Upgraded Whale Optimization Algorithm for fuzzy logic-based vibration control of nonlinear steel structure. *Eng Struct* 192:53–70. <https://doi.org/10.1016/j.engstruct.2019.05.007>
- Azizi M et al (2020) Optimization of fuzzy controller for nonlinear buildings with improved charged system search. *Struct Eng Mech* 76(6):781–797
- Bathaei A et al (2018) Semi-active seismic control of an 11-DOF building model with TMD+ MR damper using type-1 and-2 fuzzy algorithms. *J Vib Control* 24(13):2938–2953. <https://doi.org/10.1177/1077546317696369>

- Castillo O et al (2016) A comparative study of type-1 fuzzy logic systems, interval type-2 fuzzy logic systems and generalized type-2 fuzzy logic systems in control problems. *Inf Sci* 354:257–274. <https://doi.org/10.1016/j.ins.2016.03.026>
- Faravelli L, Yao T (1996) Use of adaptive networks in fuzzy control of civil structures. *Comput-Aided Civ Infrastruct Eng* 11(1):67–76
- Golnargesi S et al (2018) Seismic control of buildings with active tuned mass damper through interval type-2 fuzzy logic controller including soil–structure interaction. *Asian J Civ Eng* 19(2):177–188. <https://doi.org/10.1007/s42107-018-0016-5>
- Gómez-Skarmeta AF, Jiménez F (1999) Fuzzy modeling with hybrid systems. *Fuzzy Sets Syst* 104(2):199–208. [https://doi.org/10.1016/S0165-0114\(97\)00206-6](https://doi.org/10.1016/S0165-0114(97)00206-6)
- Holland JH (1992) *Adaptation in natural and artificial systems: an introductory analysis with applications to biology, control, and artificial intelligence*, MIT press
- Housner GW et al (1997) Structural control: past, present, and future. *J Eng Mech* 123(9):897–971. [https://doi.org/10.1061/\(ASCE\)0733-9399\(1997\)123:9\(897\)](https://doi.org/10.1061/(ASCE)0733-9399(1997)123:9(897))
- Humaidi AJ et al (2021) Social spider optimization algorithm for tuning parameters in PD-like Interval Type-2 Fuzzy Logic Controller applied to a parallel robot. *Measur Control* 54(3–4):303–323. <https://doi.org/10.1177/0020294021997483>
- Jung H-J et al (2004) State-of-the-art of semiactive control systems using MR fluid dampers in civil engineering applications. *Struct Eng Mech* 17(3–4):493–526. https://doi.org/10.12989/sem.2004.17.3_4.493
- Kang J-W, Kim H-S (2010) Fuzzy hybrid control of a wind-excited tall building. *Struct Eng Mech* 36(3):381–399. <https://doi.org/10.12989/sem.2010.36.3.381>
- Karamodin A et al (2012) Effectiveness of a fuzzy controller on the damage index of nonlinear benchmark buildings. *Sci Iran* 19(1):1–10. <https://doi.org/10.1016/j.scient.2011.12.002>
- Karnik NN, Mendel JM (2001) Centroid of a type-2 fuzzy set. *Inf Sci* 132(1–4):195–220. [https://doi.org/10.1016/S0020-0255\(01\)00069-X](https://doi.org/10.1016/S0020-0255(01)00069-X)
- Liang Q, Mendel JM (2000) Interval type-2 fuzzy logic systems: theory and design. *IEEE Trans Fuzzy Syst* 8(5):535–550. <https://doi.org/10.1109/91.873577>
- Mendel J et al (2014) *Introduction to Type-2 fuzzy logic control: theory and applications*. John Wiley & Sons
- Ohtori Y et al (2004) Benchmark control problems for seismically excited nonlinear buildings. *J Eng Mech* 130(4):366–385. [https://doi.org/10.1061/\(ASCE\)0733-9399\(2004\)130:4\(366\)](https://doi.org/10.1061/(ASCE)0733-9399(2004)130:4(366))
- Paul S et al (2018) Bidirectional active control of structures with type-2 fuzzy PD and PID. *Int J Syst Sci* 49(4):766–782. <https://doi.org/10.1080/00207721.2017.1421724>
- Rahgozar N et al (2022) Structural optimization of vertical isolated rocking core-moment frames. *J Vib Control*. <https://doi.org/10.1177/10775463221096882>
- Pourzeynali S et al (2007) Active control of high-rise building structures using fuzzy logic and genetic algorithms. *Eng Struct* 29(3):346–357. <https://doi.org/10.1016/j.engstruct.2006.04.015>
- Samali B et al (2004) Active control of cross wind response of 76-story tall building using a fuzzy controller. *J Eng Mech* 130(4):492–498. [https://doi.org/10.1061/\(ASCE\)0733-9399\(2004\)130:4\(492\)](https://doi.org/10.1061/(ASCE)0733-9399(2004)130:4(492))
- Shariatmadar H, Razavi HM (2014) Seismic control response of structures using an ATMD with fuzzy logic controller and PSO method. *Struct Eng Mech* 51(4):547–564
- Soong TT (1988) State-of-the-art review: active structural control in civil engineering. *Eng Struct* 10(2):74–84. [https://doi.org/10.1016/0141-0296\(88\)90033-8](https://doi.org/10.1016/0141-0296(88)90033-8)
- Spencer BF, Nagarajaiah S (2003) State of the art of structural control. *J Struct Eng* 129(7):845–856. [https://doi.org/10.1061/\(ASCE\)0733-9445\(2003\)129:7\(845\)](https://doi.org/10.1061/(ASCE)0733-9445(2003)129:7(845))
- Wu D (2012) On the fundamental differences between interval type-2 and type-1 fuzzy logic controllers. *IEEE Trans Fuzzy Syst* 20:832–848. <https://doi.org/10.1109/TFUZZ.2012.2186818>
- Wu D, Mendel JM (2010) Computing with words for hierarchical decision making applied to evaluating a weapon system. *IEEE Trans Fuzzy Syst* 18(3):441–460. <https://doi.org/10.1109/TFUZZ.2010.2043439>
- Wu D, Mendel JM (2019) Recommendations on designing practical interval type-2 fuzzy systems. *Eng Appl Artif Intell* 85:182–193
- Zadeh LA (1965) Fuzzy sets. *Inf control* 8(3):338–353. [https://doi.org/10.1016/S0019-9958\(65\)90241-X](https://doi.org/10.1016/S0019-9958(65)90241-X)
- Zadeh LA (1975) The concept of a linguistic variable and its application to approximate reasoning-III. *Inf Sci* 9(1):43–80. [https://doi.org/10.1016/0020-0255\(75\)90017-1](https://doi.org/10.1016/0020-0255(75)90017-1)

Springer Nature or its licensor (e.g. a society or other partner) holds exclusive rights to this article under a publishing agreement with the author(s) or other rightsholder(s); author self-archiving of the accepted manuscript version of this article is solely governed by the terms of such publishing agreement and applicable law.